Original Manuscript

SHM Structural Health Monitoring

Structural Health Monitoring
1–11

DOI: 10.1177/1475921715599050
shm.sagepub.com
SAGE

An improved fractal prediction model for forecasting mine slope deformation using GM (1, 1)

Hao Wu[1,2], Yuanfeng Dong[1], Wenzhong Shi[2], Keith C Clarke[3], Zelang Miao[2], Jianhua Zhang[1] and Xijiang Chen[1]

Abstract

The forecasting slope deformation potential is required to evaluate slope safety during open-pit mining, allowing us to formulate and promote effective emergency strategies in advance to prevent slope failure disasters. Although fractal models have been used to predict slope deformation, such limitations as low prediction accuracy, poor stability and the requirement for large amounts of data must be overcome. This article proposes an improved fractal model to forecast mine slope deformation using the grey system theory. The GM (1, 1) model is used in the improved fractal model to optimize the fitting function of the fractal dimension because of its high computational efficiency and strong fitting ability. Data sequences spanning 13 days from 11 global positioning system monitoring stations in the Jinduicheng open-pit mine in Shaanxi Province, China, were applied to forecast the slope deformation. The results from both the traditional fractal model and the improved fractal model can accurately forecast the slope deformation value fairly close to the actual field monitoring value, but the latter can make a more accurate prediction than the former. There is a significant relationship between the prediction accuracy and the data sequence dispersion. Further analysis revealed that our improved fractal model is more capable of resisting the volatility existing in the data sequences than the traditional fractal model. These findings assist in understanding the applicability of prediction models and the deformation trends of open-pit mine slopes.

Keywords

Open-pit mine, slope deformation, prediction model, fractal, GM (1, 1), global positioning system

Introduction

In numerous manufactured and natural structures, such as mountains, deep foundation pits, open-pit mines and dams, long-term deformations exist that occasionally fail as a result of complex conditions.[1] A slope failure at an open-pit mine represents the most serious and frequent hazard. Numerous mines adopt steep slope mining to improve the efficiency of mining, which leads to an increase in both the slope angle and the relative vertical slope height.[1–3] This inevitably poses potential safety hazards from mining landslides during production. Although the monitoring of high slope mines has become an integral part of mining operations,[4] the accurate prediction of mine slope deformation is important to establish effective emergency strategies in advance to reduce economic losses and loss of human life.[5]

Mathematical prediction models have been applied to forecast mine slope deformation. Lu and Rosenbaum[6] attempted to combine the artificial neural network (ANN) and grey systems to predict mine slope stability. Ferentinou and Sakellariou[7] illustrated the application of computational intelligence tools for slope deformation prediction under both static and dynamic conditions. Zhou et al.[8] described a two-dimensional plane-strain numerical model for the displacement prediction of loose soil slope. Subsequently, Li et al.[2] used the Kalman filtering model to forecast

[1]School of Resources and Environmental Engineering, Wuhan University of Technology, Wuhan, P.R. China
[2]Department of Land Surveying and Geo-Informatics, The Hong Kong Polytechnic University, Kowloon, Hong Kong
[3]Department of Geography, University of California–Santa Barbara, Santa Barbara, CA, USA

Corresponding author:
Hao Wu, School of Resources and Environmental Engineering, Wuhan University of Technology, Wuhan 430070, P.R. China.
Email: haowu1977@163.com

the high and steep mine slope deformation in the Shuichang iron mine. Feng et al. and Guo et al. expanded grey-based methods for slope stability analysis of an open-pit mine using GM (1, N) and GM (1, 1).[9–13] Recently, some extended methods have been introduced to forecast mine slope deformation. For instance, a geographic information system (GIS)-based three-dimensional (3D) limit equilibrium model was implemented by Jia et al.[14] to assess the slope stability of a mine area in Japan. Li et al.[15] presented a hybrid model combining mathematical morphology (MM) and functional-coefficient autoregressive (FAR) for slope displacement prediction. The Revised Universal Soil Loss Equation (RUSLE) model was introduced by Yellishetty et al.[16] to an abandoned opencast mine to estimate the amounts of soil landslide from mine waste rock dumps in India. Li et al.[17] used the fuzzy mathematics model to predict the deformation on rock slope of opencast metal mine. It has become common practice to use the mathematical prediction models to evaluate mine slope deformation.[18] Despite these highlighted contributions from mine slope deformation prediction models, no substantial research has yet comprehensively attempted to overcome the limitations of low prediction accuracy, poor stability, inefficient predictions using existing monitoring data with nonlinear and chaotic characteristics and the requirement for large amounts of data.[19–21]

In terms of nonlinear and chaotic features, mine slope deformation is regarded as a complex evolution system resulting from the excavation process.[22] Because of the similarity and randomness, these features of mine slope deformation can be measured using the fractal dimension, which has been thoroughly explored in previous studies.[23–25] It has been demonstrated that the fractal model has the potential to predict dynamic tendencies based on a series of existing monitoring data.[26,27] Fu[28] utilized a conventional fractal model to forecast the marine environment data, which demonstrated the advantages of the fractal dimension in nonlinear or chaotic predictions. Wu et al.[26] applied the chaos and fractal models to water quality time series predictions. A coupling model based on a variable-dimension fractal and an ANN was proposed by Qin et al.[29] to predict mine slope deformation. Qin et al. explored the use of the variable-dimension fractal method for the high rock-slope deformation research at the Xiao wan Hydropower Project; this approach was shown to be efficient.[30–32] These studies show that the fractal model can quantify the changes and trends of existing sample data. However, the fractal-based prediction model remains limited because a large quantity of sample data from continuous observation is usually unavailable.[21] Consequently, it is necessary to use certain strategies to improve the traditional fractal model (TFM) so it can be used for limited data prediction under minimal information loss.

In this article, we propose an improved fractal prediction model for forecasting mine slope deformation using GM (1, 1). The fitting correction of the fractal dimension is optimized using GM (1, 1) for the existing variable-dimension fractal model. This article is organized as follows: section 'Methodology' reviews the original variable-dimension fractal model and the GM (1, 1), and then the improved fractal prediction model is detailed. A study area and data collection method using global positioning system (GPS) is introduced in section 'Study area and data'. In section 'Results', we use the improved fractal prediction model to forecast mine slope displacement, comparing its results with that of the original variable-dimension fractal model. Finally, the conclusion is presented.

Methodology

Fractal model

The term fractal was derived from the Latin word 'fractus' by Mandelbrot.[33] The fractal can bridge the similarity between a part and the whole, and emphasizes the global dependence to part fractal along the direction from microscopic to macroscopic.[33,34] Both self-similarity and randomness are the basic fractal characteristics. They can be well quantified by the fractal dimensions that have been extended from the integer dimensions. Although they neither uniquely describe nor specify details of how to construct particular fractal patterns, it has been shown that the fractal dimensions are fitted to quantify the nonlinear characteristics.[21,26]

Mine slope deformation is a complex system affected by external environmental changes, the evolution of which shows complex irregular trends. This deformation is characterized by the self-similarity in a statistical sense.[35] Yang et al.[36] have indicated that the mine slope deformation has rheological characteristics and creep behaviour of the northern slope of an open-pit mine in Fushun City, Liaoning Province, China. Thus, the monitoring data of mine slope deformation are a series of discrete points with fractal features related to time.[37] Actually, the fractal model is suitable for forecasting mine slope deformation because of its self-similarity and powerful fitting ability for different deformation trends.[33] The fractal model has been used to predict slope deformation since the 1990s. Zhang and Mao proposed the initial slope fractal model to analyse landslide deformation.[38,39]

In practical application, the general function of fractal model can be expressed by the power exponent distribution as follows

$$N = \frac{C}{r^D} \tag{1}$$

where r is the characteristic linear scale, C is the unknown constant and N is the number of objects at scale r, such as temperature, stress value and the deformation value. D is the fractal dimension that can measure the complexity and randomicity.

To observe the mine slope deformation, we numbered the monitoring time as $r(r = 1, 2, \ldots, n)$ and defined the mine slope deformation value as $N(N = 1, 2, \ldots, n)$. Thus, we can derive a series of spatial-temporal coordinate pairs of mine slope deformation, including $(N_1, r_1), (N_2, r_2), \ldots, (N_i, r_i), (N_j, r_j), \ldots, (N_n, r_n)$. The fractal functions at time i and j can be expressed as follows

$$\ln N_i = \ln C - D \ln r_i \tag{2}$$

$$\ln N_j = \ln C - D \ln r_j \tag{3}$$

We can then use the variable-dimension fractal to build the interaction function at different monitoring periods.[23,26] The variable-dimension fractal dimension was derived from equations (2) and (3) as follows

$$D_{(i,j)} = \frac{\ln\ (N_i/N_j)}{\ln\ (r_j/r_i)} \tag{4}$$

where $D_{(i,j)}$ is the variable-dimension fractal dimension. In general, we make use of the cumulative sum sequences of the original observations to solve this problem. The building of cumulative sum sequences has been expressed in detail by Wu et al.[26] According to equation (4), the fractal dimension sequence can be determined as follows

$$D(I)_{(i,\,i+1)} = \frac{\ln\ (S(I)_{i+1}/S(I)_i)}{\ln\ (r_i/r_{i+1})} \tag{5}$$

where $D(I)_{(i,\,i+1)}$ is the corresponding fractal dimension of the I-order cumulative sum and r_i is the monitoring time sequence. $S(I)_i$ is the cumulative sum sequences that can be built from the monitoring data sequence.[40,41] A detailed computation of fractal dimensions was performed by Wu et al.[26]

After the calculation of the fractal dimension, the mine slope deformation N_{i+1} can be obtained as follows

$$N_{i+1} = S(I)_{i+1} - (N_i + N_{i-1} + \cdots + N_2 + N_1) \tag{6}$$

where $N_1, N_2, \ldots, N_{i-1}, N_i$ is the monitoring data sequence, and N_{i+1} is the mine slope deformation value at time $i+1$.

Although the fractal dimension has the potential to describe the dynamic tendency of slope deformation based on an existing monitoring data series, as discussed above, the question of how to use the fractal model to accurately predict the mine slope deformation with limited monitoring data remains largely unanswered.[21] In addition, the TFM is sensitive to the timeliness and continuity of the monitoring data series,[28] which lead to the limitations in the practical application of this model. Systematic improvements to the accurate application of the fractal model are required, particularly because it is difficult to obtain a continuous series of long-term monitoring data and make timely predictions based on short-term monitoring data.

Grey prediction model

The fractal model can accurately predict slope deformation as stated above, but its application is restricted because of the large amount of data required. Several other mathematical models have been applied to slope deformation predictions. For example, the grey system theory is a classical prediction model that was initially introduced in 1982. It has since become popular because it can simulate the systems with objective uncertainty and imperfect known data.[42] Due to its computational efficiency,[43] the GM (1, 1) type of grey prediction model has been widely applied in practice, rather than conventional statistical models such as regression analysis model, time series analysis model and Kalman filtering model.[44,45] Consequently, we utilized the GM (1, 1) to fit the forecast fractal dimensions and to address the large amounts of data required by the fractal model previously mentioned in this article.

The grey prediction model involves the following three basic operations: (1) the accumulated generating operator (AGO), (2) the construction of background value matrix and (3) the calculation of the developing coefficient a and the grey controlled variable b. When the original data series are acquired, the AGO series can be built. A detailed building of AGO series was performed by Chang et al.[45] Its first-order differential equation can be expressed as follows

$$\frac{dX^{(1)}}{dt} + aX^{(1)} = b \tag{7}$$

where t is the independent variable. Both the developing coefficient a and the grey controlled variable b were calculated using the ordinary least-square method. The parameters a and b can be calculated through the accumulated matrix and a detailed description of accumulated matrix was performed by Chang et al.[45]

The values of a and b were then input into equation (7) to discretize the differential equation. The desired prediction output at time $K+1$ can be estimated by an inverse AGO, which was determined by the following relation

$$x^{(0)}(k+1) = x^{(1)}(k+1) - x^{(1)}(k) = (1 - e^{a})\left(x^{(0)}(1) - \frac{a}{b}\right)e^{-ak} \tag{8}$$

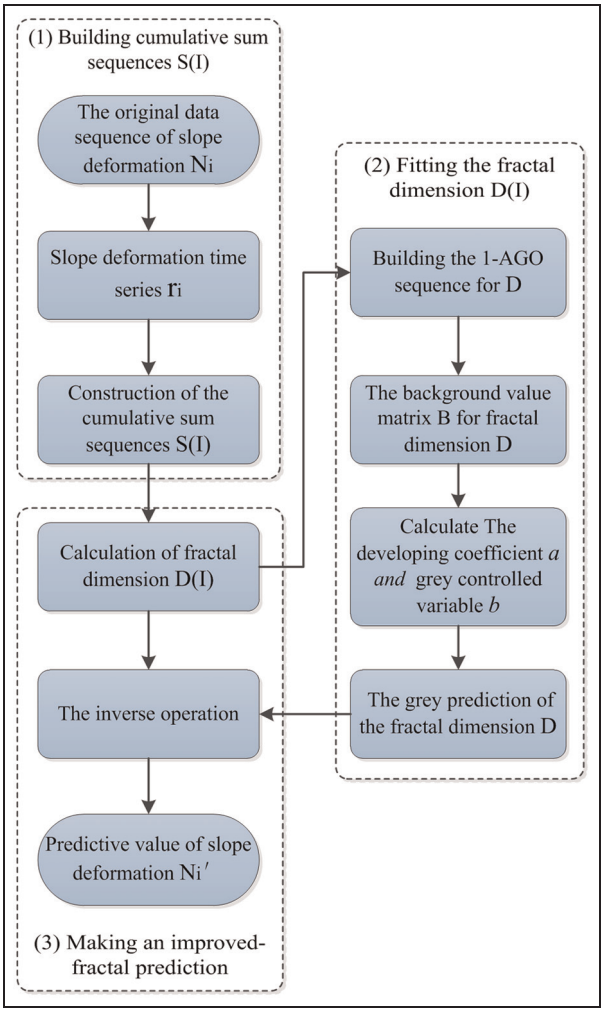

Figure 1. Flowchart of the improved fractal prediction model.

where $x^{(0)}(1) = x^{(1)}(1)$, $x^{(0)}(k+1)$ is the grey elementary forecasting value. The characteristic behaviour of the GM (1, 1) is generally described by discrete time series data.[46]

Improved fractal prediction model using GM (1, 1)

To achieve a high prediction accuracy for mine slope deformation, a novel mine slope deformation prediction model is derived from and substituted for the existing variable-dimension fractal model. Compared to the existing literature, the focus of our work is to fit the forecast fractal dimensions using the GM (1, 1). The entire procedure and flow is shown in Figure 1.

The improved fractal prediction model using GM (1, 1) shown in Figure 1 pertains to the existing variable-dimension fractal model. The traditional method of fractal dimension-fitting results in erroneous prediction results when the monitoring data are limited. Thus, the GM (1, 1) was utilized to fit the forecast fractal dimension given small samples and poor information. The three key steps of the proposed improved fractal prediction model are as follows:

Step 1. The cumulative sum sequences $S(I)$ were built from the original data series. Using the cumulative sum sequence transformation, the original data series can better meet the requirements of the fractal model as described by Wu et al.[26]

Step 2. When the fractal dimension series $D(I)_{(1,2)}$, $D(I)_{(2,3)}, \ldots, D(I)_{(i,\,i+1)}$ were derived from equation (5), the GM (1, 1) was integrated into the TFM to fit the forecast fractal dimension $D(I)_{(i+1,\,i+2)}$ instead of the exponent equation. This is the core part of the improved prediction model.

Step 3. The mine slope deformation values at time $i+1$ were forecasted. According to equation (6), we used the inverse extrapolation to predict the mine slope deformation.

Study area and data

Study area

The Jinduicheng Molybdenum Mining Corporation, shown in Figure 2(a), has a mining area of 4.5 km^2 in the Shaanxi Province of northwest of China. It is the largest molybdenum production base in China and ranks among the top three in the world. The Jinduicheng molybdenum mine has utilized open-pit mining for production since 1950s. With the continuous exploitation and rapid advances in mining technology in recent years, it is now characterized by high and steep slopes as shown in Figure 2(b). However, these high and steep slopes present a serious threat to safe production in the entire mining area. Thus, managers and workers must establish effective monitoring measures and an accurate prediction model to forecast slope deformation tendencies as soon as possible.

The northern slope of the Jinduicheng open-pit mine shown in Figure 2(a) was selected as our study area. An artificially high slope has now formed on the northern slope. This slope is approximately 650 m long and 150–170 m high with a 40° slope angle. Because the Yan door geological fault zone exactly crosses through the northern slope, the rock mass in this area is loose and lacks stability. Consequently, small-scale slope failures occur. During the rainy season, the surface water permeates through the permeable layer and secondary geological disasters are triggered.

Data

The data sequence used in our experiment was collected through GPS monitoring stations placed at the

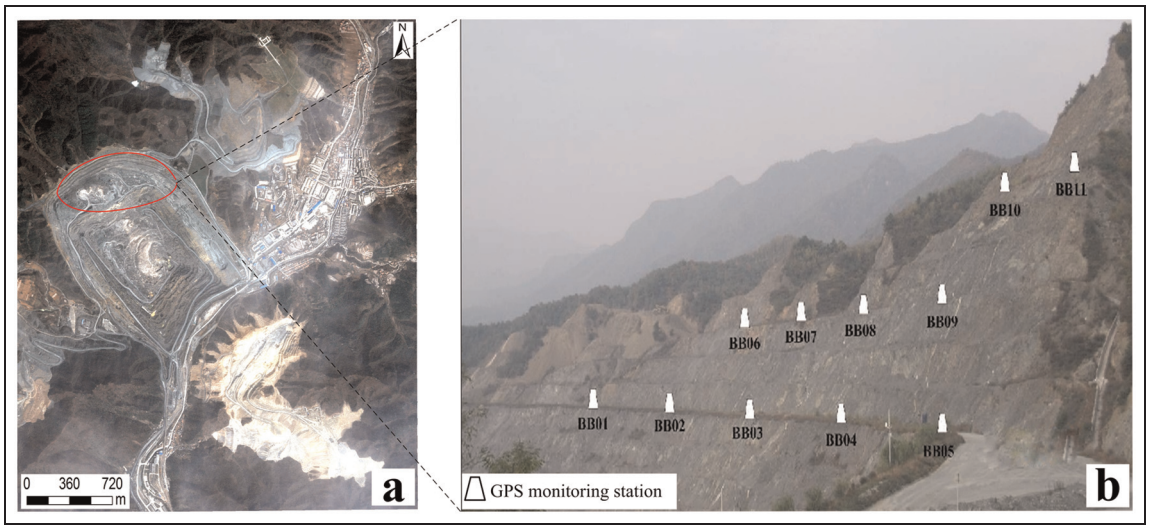

Figure 2. Location of study area and the arrangement of GPS monitoring stations: (a) the area labelled the red circle is our study area covered the northern slope and (b) 11 GPS monitoring stations on the northern slope are arranged at three different layers that has about 30 m interval in height.

northern slope, as shown in Figure 2(b). The GPS is a space-based satellite navigation system that can provide location and time information in all weather conditions.[47] It was developed by the US Department of Defense and put into use in April 1993. There are currently more than 20 satellites in orbit, normally providing global coverage. For any outdoor point on the earth, the GPS receiver can simultaneously observe four or more GPS satellites, guaranteeing all-weather and anywhere navigation and 3D positioning.[48]

The GPS has been used to monitor mine slope deformation since the late 1990s because of its high precision, automation and all-weather adaptability compared with other optical surveying equipment.[49] In 2012, a GPS-based automatic monitoring system was designed and installed to monitor the slope deformation of the northern slope. This system includes three main parts: the data acquisition element (the 11 GPS monitoring stations shown in Figure 2(b)), the data transmission element and the GPS data processing element. Although data acquisition has become convenient and timely with the support of GPS, the original GPS data could only describe past slope deformation rather than predicting future deformation trends. Future slope deformation trends are unknown to managers and workers. Therefore, we must analyse the original deformation data using appropriate mathematical prediction models.

In this article, the height observations from the GPS monitoring stations are used to validate and evaluate the proposed model because deformation in the height direction of the slope can result in slope failure in the mining area. We collected the time series data from 11 monitoring stations from 6 July 2013 to 18 July 2013. The cumulative displacement time series reference for all stations listed in Table 1 was taken on 5 July 2013. The observation data from 6 July to 15 July were used to train the proposed model, and the observation data from 16 July to 18 July were used to validate the prediction accuracy (marked with * in Table 1).

Analysis of nonlinear property of data sequences based on R^2

As mentioned above, mine slope deformation is regarded as a complex evolution system and shows nonlinear and chaotic characteristics. The original data sequence collected from the GPS stations is able to reflect these characteristics. We also elaborated that the fractal model is suitable for fitting forecast these monitoring data sequence with nonlinear and chaotic characteristics. Thus, it is very necessary for us to verify the nonlinearity of the data sequence before using our proposed model to predict slope deformation.

In statistics, the coefficient of determination, denoted as R^2, is an indicator to quantify how well datasets fit a statistical model.[50] Generally, the coefficient of determination ranges from 0 to 1. In few extreme circumstances, the computational definition of R^2 can yield negative values, but it rarely occurs. If the value of R^2 is closer to 1, it means the better fitting degree, and vice versa.[51] Linear fitting is very poor if the value of R^2 lies between 0 and 0.5. We have written a programme in the software of MATLAB to fit the data series with best statistical model automatically.

Table 1. Height observations of cumulative displacement on 6 July 2013 to 18 July 2013 were collected from 11 GPS monitoring stations that were installed at the northern slope of Jinduicheng open-pit mine shown in Figure 2(b).

Date (mm/dd/yyyy)	The observations of cumulative displacement for monitoring stations (m)										
	BB01	BB02	BB03	BB04	BB05	BB06	BB07	BB08	BB09	BB10	BB11
07/06/2013	−0.0353	−0.0214	−0.0240	−0.0310	−0.0588	−0.0429	−0.0586	−0.0443	−0.0383	−0.0834	−0.0378
07/07/2013	−0.0329	−0.0271	−0.0327	−0.0343	−0.0653	−0.0546	−0.0544	−0.0600	−0.0412	−0.0887	−0.0737
07/08/2013	−0.0002	−0.0113	−0.0185	−0.0250	−0.0469	−0.0390	−0.0378	−0.0412	−0.0313	−0.0796	−0.0671
07/09/2013	−0.0459	−0.0146	−0.0243	−0.0449	−0.0736	−0.0549	−0.0634	−0.0937	−0.0558	−0.0954	−0.0528
07/10/2013	−0.0634	−0.0564	−0.0559	−0.0657	−0.1025	−0.0871	−0.0839	−0.0861	−0.0523	−0.0974	−0.0723
07/11/2013	−0.0415	−0.0815	−0.0242	−0.0418	−0.0780	−0.0562	−0.0560	−0.1127	−0.0561	−0.0871	−0.0570
07/12/2013	−0.0532	−0.0835	−0.0430	−0.0407	−0.0874	−0.0654	−0.0669	−0.1016	−0.0582	−0.0743	−0.0648
07/13/2013	−0.0523	−0.0346	−0.0380	−0.0436	−0.0921	−0.0799	−0.0775	−0.0666	−0.0518	−0.0952	−0.1043
07/14/2013	−0.0674	−0.0399	−0.0416	−0.0456	−0.0999	−0.0868	−0.0849	−0.0845	−0.0502	−0.1079	−0.0730
07/15/2013	−0.0860	−0.0495	−0.0477	−0.0573	−0.0722	−0.0875	−0.0710	−0.0998	−0.0528	−0.1048	−0.0400
07/16/2013*	−0.0956	−0.0511	−0.0464	−0.0418	−0.1181	−0.1024	−0.0902	−0.0929	−0.0510	−0.0939	−0.0327
07/17/2013*	−0.1137	−0.0675	−0.0483	−0.0464	−0.1041	−0.1151	−0.0937	−0.0994	−0.0617	−0.1035	−0.0624
07/18/2013*	−0.1216	−0.0731	−0.0524	−0.0421	−0.1285	−0.1262	−0.1062	−0.0918	−0.0622	−0.0993	−0.0603

GPS: global positioning system.
*Observation data from 16 July to 18 July were used to validate the prediction accuracy rather than to train the proposed model in our experiment.

Table 2. Comparison of R^2 values of Gaussian fitting and linear fitting for raw data sequences.

R^2	R^2 values of original data sequences for 11 monitoring stations										
	BB01	BB02	BB03	BB04	BB05	BB06	BB07	BB08	BB09	BB10	BB11
Gaussian fitting	0.9209	0.9624	0.9626	0.9223	0.9755	0.9478	0.897	0.9506	0.9529	0.977	0.974
Linear fitting	0.3057	0.00926	0.5214	0.1583	0.04869	0.05457	0.6927	0.3883	0.05225	0.364	0.0031

The results indicate that the Gaussian fitting with power law characteristics had the best fitting degree (the value of R^2 is closer to 1) as shown in Table 2. The R^2 value of Gaussian fitting is greater than 0.9 except BB07. This suggests that these monitoring data sequences can be well fitted with nonlinear fitting function, and the strong nonlinear characteristics are proved to exist in the data sequences. At the same time, the R^2 values of linear fitting are also listed in Table 2 in sharp contrast to the Gaussian fitting. The R^2 value of linear fitting is less than 0.4 except BB03 and BB07. It indicates that the data sequence has weak linear characteristics in statistics. A distinct nonlinear feature can be found in these monitoring data sequences through the verification of Gaussian fitting and linear fitting in pros and cons.

Results

The calculation results of fractal dimension for TFM and improved fractal model (IFM) are shown in Table 3, from 16 July 2013 to 18 July 2013. These prediction dimensions are used to predict the mine slope deformation through the inverse extrapolation. They were calculated using the MATLAB software (version 7.8).

Table 4 shows the predicted slope deformation results derived from the TFM and the IFM presented in section 'Methodology'. All of the predicted slope deformation values for the 11 monitoring stations from 16 July 2013 to 18 July 2013 are positive. This suggests that the northern slope tends to be unstable and a series of deformation phenomena could arise on the potential slip surface. For each of monitoring stations, there is a gradual change in the predicted deformation value from 16 July to 18 July. The deformation value of BB01 for TFM and IFM increased from 0.0833 to 0.0947 m and from 0.1042 to 0.1494 m, respectively. This indicates that the slope instability becomes evident gradually during these few days. The deformation values for a given day presented in Table 4 show no correlation among the 11 monitoring stations compared with the actual deformation values. This may be attributed to the geological structural differences beneath each monitoring station. For the majority of monitoring stations, the forecast sequence appears gentle with a gradually increasing trend, indicating a continuous deformation and a slow creep state. However, as shown

Table 3. Prediction results of fractal dimension for the traditional fractal model (TFM) and the improved fractal model (IFM) on 07/16/2013, 07/17/2013 and 07/18/2013.

Monitoring stations	TFM			IFM		
	07/16/2013	07/17/2013	07/18/2013	07/16/2013	07/17/2013	07/18/2013
BB01	0.0832	0.0891	0.0947	0.1477	0.1354	0.1669
BB02	0.0709	0.0755	0.0799	0.0655	0.0695	0.0736
BB03	0.0482	0.0502	0.0521	0.0553	0.0607	0.0667
BB04	0.0559	0.0496	0.0501	0.0563	0.0586	0.0611
BB05	0.0951	0.0969	0.0986	0.0995	0.1033	0.1073
BB06	0.0952	0.1003	0.1055	0.1043	0.1141	0.1149
BB07	0.0807	0.0825	0.0841	0.0912	0.0974	0.1042
BB08	0.1035	0.1063	0.1089	0.1014	0.1038	0.1055
BB09	0.0574	0.0583	0.0592	0.0594	0.0611	0.0628
BB10	0.1058	0.1088	0.1184	0.1047	0.1073	0.1099
BB11	0.1322	0.1488	0.1677	0.0961	0.0985	0.1008

Table 4. Forecast results of the traditional fractal model (TFM) and the improved fractal model (IFM) from 16 July 2013 to 18 July 2013.

Monitoring stations	07/16/2013		07/17/2013		07/18/2013	
	TFM (m)	IFM (m)	TFM (m)	IFM (m)	TFM (m)	IFM (m)
BB01	0.0833	0.1042	0.0891	0.1245	0.0947	0.1494
BB02	0.0710	0.0656	0.0755	0.0696	0.0800	0.0736
BB03	0.0545	0.0453	0.0494	0.0485	0.0513	0.0518
BB04	0.0559	0.0430	0.0497	0.0456	0.0501	0.0459
BB05	0.0951	0.0995	0.0969	0.1034	0.0986	0.1073
BB06	0.0951	0.1043	0.1003	0.1141	0.1055	0.1250
BB07	0.0808	0.0912	0.0825	0.0974	0.0840	0.1042
BB08	0.1036	0.1014	0.1064	0.1038	0.1099	0.1061
BB09	0.0575	0.0595	0.0584	0.0612	0.0592	0.0629
BB10	0.1058	0.1047	0.1090	0.1073	0.1118	0.1100
BB11	0.0118	0.0146	0.1022	0.0575	0.0867	0.0557

in Table 4, BB11 shows a random variation with large fluctuations; this area needs to be specifically monitored. It is noted that the forecast results for TFM or IFM shown in Table 4 indicate the cumulative values of slope deformation. In comparison with the available actual deformation values, it is more important for us to capture the ongoing ground movement caused by the mining process as soon as possible.

Discussion

Significance test of the proposed model

Previous studies have confirmed that the TFM is capable of forecasting the slope deformation from the time series data.[29,30,33] However, as a new type of combination prediction model, the IFM proposed in this article must be validated in practice. Thus, we applied the student's *t*-test to examine whether our IFM was an effective tool to accurately predict the actual deformation value. A null hypothesis of statistical probability was defined because the forecast deformation value does not approximate the actual deformation value. If the statistical test results reject the null hypothesis, the forecast deformation is close to the actual deformation; this suggests that the prediction model has a greater forecast error and its accuracy is relatively low. All significance tests for the proposed model were performed using the SPSS software.

Figure 3 shows that the majority of the statistical tests for the predicted deformation values from 16 July to 18 July are significant at the 0.01 level. This suggests that the mean of the population has the value specified in the above-mentioned null hypothesis. That is, there is no difference between the predicted and actual values. Both prediction models (i.e. the TFM and the IFM) can predict the slope deformation value fairly close to the actual field monitoring value. This indicates that

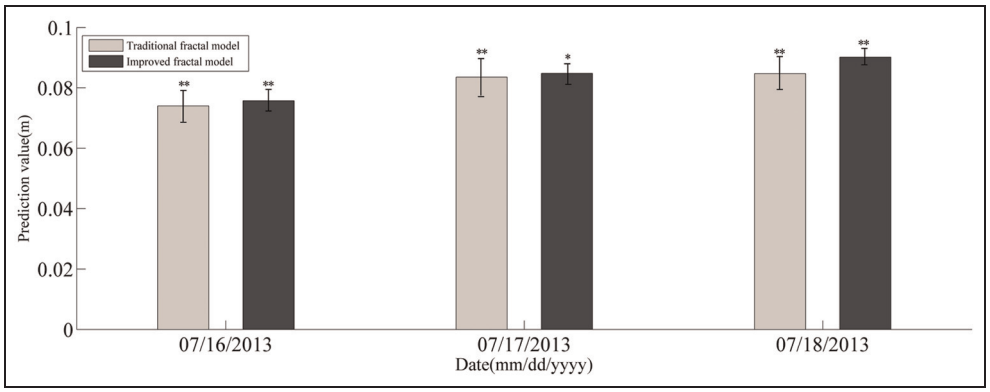

Figure 3. Results of significance test for the traditional fractal model and the improved fractal model. The symbol (**) denotes that the correlation is significant at the 0.01 level (two-tailed) while symbol (*) at the 0.05 level (two-tailed).

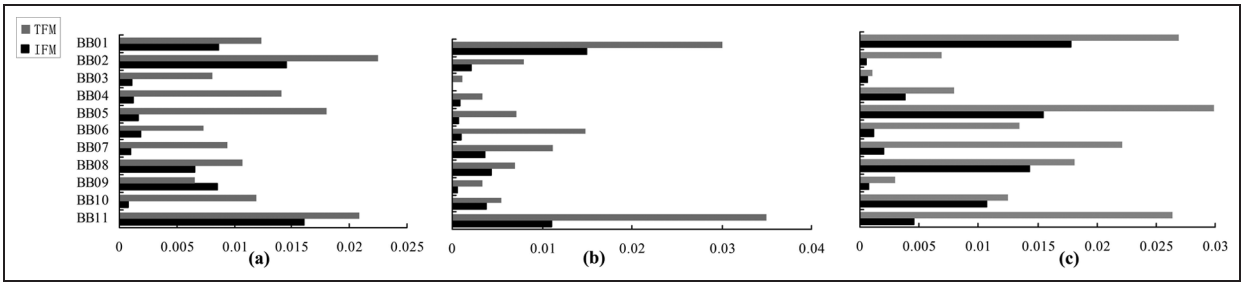

Figure 4. Comparison of absolute residuals between the traditional fractal model (TFM) and the improved fractal model (IFM) on (a) 07/16/2013, (b) 07/17/2013 and (c) 07/18/2013.

our proposed model can achieve acceptable accuracy compared to the TFM. However, it is noted that the statistical test for the improved fractal prediction values on 17 July is significant at the 0.05 level rather than at the 0.01 level, indicating a low forecast accuracy for this period. We speculate that this may correspond to an abrupt large fluctuation among the data sequences. This may have resulted from a sudden and heavy rain on 17 July causing the slope deformation situation to be different from the other two days. However, we cannot completely rule out the possibility that it may also be a result of random error and stochastic uncertainty in the original data sequence, which can also lead to a low significance.

Comparison of the prediction accuracy of the TFM and our IFM

The aforementioned results indicate that our IFM can predict the slope deformation from the existing monitoring data as well as the TFM can. However, it is performed only at the general level of student's *t*-test, rather than at each specific monitoring station. We need to conduct comparative analyses for each monitoring station to validate the superior deformation forecasting performance of our proposed improved fractal prediction model over that of the TFM. The differences between actual observation values and predictive values for two kinds of prediction model, including the TFM and the IFM, are shown in Figure 4. It shows that IFM has a smaller forecast error than TFM for all 11 monitoring stations from 16 July to 18 July. All IFM-derived prediction results among 11 stations have improved greatly in comparison with that of TFM. This indicates that our IFM has better prediction accuracy than the TFM. At the same time, Figure 4 shows that the absolute residuals on (c) 07/18/2013 are much bigger than the forecast error with the date of (a) 07/16/2013 and (b) 07/17/2013, which demonstrates that the more the time span, the greater forecast error is for both the TFM and IFM.

Why does our IFM result in smaller forecast errors than the TFM? This question can be explored by examining the fitting prediction of the fractal dimension. For the TFM, the exponent equation $y = ae^{-bx} + c$ was used to fit the forecast fractal dimensions. Because of the explosive growth characteristic in the exponent equation,[52] minor changes in the data sequences may result

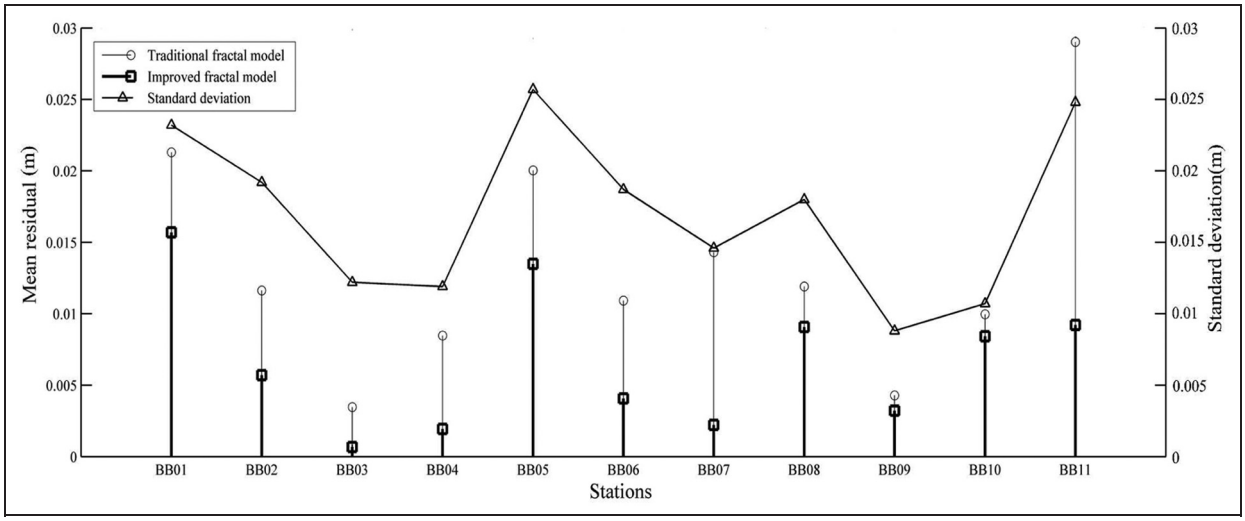

Figure 5. Relationship of the accuracy of two prediction models (the traditional fractal model and the improved fractal model) versus the dispersion of observation from 11 GPS monitoring stations. The accuracy of prediction model is plotted for the mean residual on the left axis while the dispersion of observation for the standard deviation on the right axis.

in a serious forecasting error in the fractal dimension as shown in Figure 4. Conversely, our IFM has a relatively high prediction accuracy in this study. This is primarily because of the fitting improvement of the fractal dimension using GM (1, 1). As discussed earlier, the differential equation $(dx/dt) + ax = b$ was used instead of the grey equation $x^{(0)}(k) + az^{(1)}(k) = b$ in the GM (1, 1); this equation can describe the situation when a complicated relation, involving several continuously varying quantities and changing trends in space or time, is unknown or postulated. Thus, the equation has the continuous fitting ability to simulate a system with objective uncertainty given imperfectly known data. The explosive growth occurrence probability that usually occurs in the TFM is reduced in comparison with the exponent equation. This can significantly improve the fitting prediction of the fractal dimension to achieve a more accurate slope deformation prediction.

Relationship of the prediction accuracy and the dispersion of data sequence

The forecast accuracy is not only related to prediction models but also depends on the amplitude variations of the data sequences. Figure 5 shows that there is a significant relationship between the prediction accuracy and the dispersion of data sequences. This suggests that the mean residual becomes smaller when the standard deviation is small, and vice versa. The large standard deviation generally corresponds to a high forecast error, regardless of which of the two prediction models is used. That is, the mean residual varies with the standard deviation changes. This is because the fractal dimension is sensitive to fluctuations in the data sequence or limitations in the quantity of data. However, not all monitoring station forecast errors in our study follow this rule. For instance, the change trend of forecast error at BB06 and BB07 tends to oppose the standard deviation, as shown in Figure 5. This may be a result of local geological conditions triggered by blasting vibrations in the mine slope.

The correlation coefficients between the mean residual and standard deviation for the TFM and the IFM are 0.8625 and 0.7352, respectively. This suggests that the TFM is more easily affected by the data sequence fluctuation, whereas our IFM is able to resist the volatility in the data sequences. This is beneficial in making an effective prediction in the short-term monitoring data sequences. Specifically, it works well when a sudden deformation occurs, such as in the case of rainfall or abrupt geological movement.

Conclusion

It is reported that the fractal model has the potential to forecast mine slope deformation from a series of existing monitoring data because of its similarity and randomness. However, the requirement for large quantities of data has degraded the applicability of the TFM in practice. This study proposes an IFM to forecast mine slope deformation with limited data sequences, with the fractal dimension-fitting forecast optimized by GM (1, 1). The primary conclusions from this study can be summarized as follows:

(1) A significance test suggests that the forecast value of the IFM is statistically correlated to the actual values at the macro level. It also corroborates that

the IFM is an effective tool that can predict the slope deformation value close to the real value.

(2) Comparison analysis of the mean residual suggests that our IFM can more accurately predict mine slope deformation at each monitoring station than the TFM.

(3) Although the prediction accuracies of both the TFM and the IFM are affected by the dispersion of the data sequence, a thorough analysis demonstrates that the latter is better able to resist the volatility existing in the data sequences than the former.

Despite the achievements in this research, there are currently several limitations that present opportunities for improvement in the future. For instance, the data sequences used in this study are generally sampled at equal time intervals. However, because of the collection method limitations and the influence of the external environment, most of the data sequences acquired from field monitoring are an unequal interval time series. Given the influence of continuity of time series,[42] we must conduct additional studies, using more novel methods based on the unequal interval time series, to improve the availability of data sequences. This is beneficial for researchers to understand the applicability of prediction models to apply additional multiple data sequences for forecasting mine slope deformation.

Acknowledgements

The authors are grateful to Elsevier Language Editing Services to the manuscript.

Declaration of conflicting interests

The author(s) declared no potential conflicts of interest with respect to the research, authorship and/or publication of this article.

Funding

This work was supported by the National Natural Science Foundation of China (40901214), the China Postdoctoral Science Foundation (2013M531749 and 2012T50691), the Hong Kong Scholars Program (XJ2012036), the Hong Kong Polytechnic University under Projects (G-YZ26) and the self-determined and innovative research funds of WUT (20131049708009).

References

1. Ding XL, Ren DY, Montgomery B, et al. Automatic monitoring of slope deformations using geotechnical instruments. *J Survey Eng: ASCE* 2000; 126: 57–68.
2. Li CH, Fan LP, Zhang JL, et al. Application of Kalman filtering to high and steep slope deformation monitoring prediction of open-pit mines. *J Univ Sci Tech Beijing* 2010; 32: 8–13.
3. Dwivedi RD, Singh M, Viladkar MN, et al. Prediction of tunnel deformation in squeezing grounds. *Eng Geol* 2013; 161: 55–64.
4. Bachmann D, Bouissou S and Chemenda A. Analysis of massif fracturing during deep-seated gravitational slope deformation by physical and numerical modeling. *Geomorphology* 2009; 103: 130–135.
5. Pareek N, Pal S, Sharma ML, et al. Study of effect of seismic displacements on landslide susceptibility zonation (LSZ) in Garhwal Himalayan region of India using GIS and remote sensing techniques. *Comput Geosci* 2013; 61: 50–63.
6. Lu P and Rosenbaum MS. Artificial neural networks and grey systems for the prediction of slope stability. *Natural Hazards* 2003; 30: 383–398.
7. Ferentinou MD and Sakellariou MG. Computational intelligence tools for the prediction of slope performance. *Comput Geotech* 2007; 34: 362–384.
8. Zhou YD, Cheuk CY and Tham LG. Numerical modelling of soil nails in loose fill slope under surcharge loading. *Comput Geotech* 2009; 36: 837–850.
9. Feng QS. Study of grey forecasting in slope rock mass deformation. *J Inn Mongol Univ Sci Tech* 2011; 30: 196–198.
10. Shen YF and Giurgiutiu V. WaveFormRevealer: an analytical framework and predictive tool for the simulation of multi-modal guided wave propagation and interaction with damage. *Struct Health Monit* 2014; 13: 491–511.
11. Wang FK, Hsiao YY and Chang KK. Combining diffusion and grey models based on evolutionary optimization algorithms to forecast motherboard shipments. *Math Prob Eng* 2012; 2012: 849634.
12. Guo J, Gan DQ, Zhang Y, et al. Application of GM (1, N) model on slope stability analysis in open pit mine. In: Yang A, Qu JG and Qu X (eds) *Green power, materials and manufacturing technology and applications* (pts 1 and 2). 2011, pp. 729–732. Clausthal-Zellerfeld: Trans Tech Publications.
13. Wasowski J and Bovenga F. Investigating landslides and unstable slopes with satellite multi temporal interferometry: current issues and future perspectives. *Eng Geol* 2014; 174: 103–138.
14. Jia N, Mitani Y, Xie MW, et al. Shallow landslide hazard assessment using a three-dimensional deterministic model in a mountainous area. *Comput Geotech* 2012; 45: 1–10.
15. Li QY, Xu J, Wang WH, et al. Slope displacement prediction based on morphological filtering. *J Central South Univ* 2013; 20: 1724–1730.
16. Yellishetty M, Mudd GM and Shukla R. Prediction of soil erosion from waste dumps of opencast mines and evaluation of their impacts on the environment. *Int J Min Reclam Env* 2013; 27: 88–102.
17. Li WX, Qi DL, Zheng SF, et al. Fuzzy mathematics model and its numerical method of stability analysis on rock slope of opencast metal mine. *Appl Math Model* 2015; 39: 1784–1793.
18. Du J, Yin KL and Lacasse S. Displacement prediction in colluvial landslides, Three Gorges Reservoir, China. *Landslides* 2013; 10: 203–218.

19. Luo XF, Cheng T, Li X, et al. Slope safety factor search strategy for multiple sample points for reliability analysis. *Eng Geol* 2012; 129: 27–37.
20. Kim GH, An SH and Kang KI. Comparison of construction cost estimating models based on regression analysis, neural networks, and case-based reasoning. *Build Environ* 2004; 39: 1235–1242.
21. Cui HR and Yang L. Short-term electricity price forecast based on improved fractal theory. In: *2009 international conference on computer engineering and technology*, Singapore, 22–24 January 2009, pp. 347–351. New York: IEEE.
22. Casagli N, Catani F, Del Ventisette C, et al. Monitoring, prediction, and early warning using ground-based radar interferometry. *Landslides* 2010; 7: 291–301.
23. Oestreicher C. A history of chaos theory. *Dialog Clin Neurosci* 2007; 9: 279–289.
24. Nada SI. Fractal dimension of chaotic dynamical spaces. *Chaos Solit Fracts* 2006; 30: 374–379.
25. Chu J, Yang YJ, Li YM, et al. Chaos dynamic study on slope stability problem. In: *International symposium on mining science and safety technology*, Jiaozuo, PR China, April 16–19, 2007, pp. 557–563. Beijing, PR China: Science Press Beijing.
26. Wu J, Lu J and Wang JQ. Application of chaos and fractal models to water quality time series prediction. *Env Model Softw* 2009; 24: 632–636.
27. Zhou QF, Ning YP, Zhou QQ, et al. Structural damage detection method based on random forests and data fusion. *Struct Health Monit* 2013; 12: 48–58.
28. Fu YH. Transform-formed fractals and analyses and forecast of marine environment data. *Marine Sci Bull* 2000; 19: 79–88.
29. Qin P, Zhang JY, Qin ZH, et al. IVDF-ANN prediction model for monitoring data of landslide deformation. *J Yang River Sci Res Inst* 2012; 29: 29–34.
30. Qin P and Qin ZH. Forecasting model of monitoring data of high rock slope based on improved variable dimension fractal theory. *Hydro-Sci Eng* 2010; 1: 90–94.
31. Wang XJ, Yang C, Wang L, et al. Membership-set identification method for structural damage based on measured natural frequencies and static displacements. *Struct Health Monit* 2013; 12: 23–34.
32. Lee DH, Lai MH, Wu JH, et al. Slope management criteria for Alishan Highway based on database of heavy rainfall-induced slope failures. *Eng Geol* 2013; 162: 97–107.
33. Mandelbrot BB. Fractal analysis and synthesis of fracture surface roughness and related forms of complexity and disorder. *Int J Fract* 2006; 138: 13–17.
34. Gao J, Hu J and Tung W-w. Facilitating joint chaos and fractal analysis of biosignals through nonlinear adaptive filtering. *PLoS ONE* 2011; 6: e24331.
35. Luo X, Li X, Zhou J, et al. A Kriging-based hybrid optimization algorithm for slope reliability analysis. *Struct Safe* 2012; 34: 401–406.
36. Yang T, Xu T, Liu H, et al. Rheological characteristics of weak rock mass and effects on the long-term stability of slopes. *Rock Mech Rock Eng* 2014; 47: 2253–2263.
37. Li XB and Gong FQ. A method for fitting probability distributions to engineering properties of rock masses using Legendre orthogonal polynomials. *Struct Safe* 2009; 31: 335–343.
38. Zhang ZX and Su J. Fractal block theory and its application to the high slope of the Three Gorges Project of the Yangtze River. *J Tong Univ (Nat Sci)* 1996; 24: 552–557.
39. Mao DM and Zhang F. Application of fractal geometry on forecasting the stability of the slope. *J Baot Univ Iron Steel Tech* 1999; 18: 407–410.
40. Klimstra M and Zehr EP. A sigmoid function is the best fit for the ascending limb of the Hoffmann reflex recruitment curve. *Exp Brain Res* 2008; 186: 93–105.
41. Fernandez-Martinez M and Sanchez-Granero MA. Fractal dimension for fractal structures: a Hausdorff approach revisited. *J Math Anal Appl* 2014; 409: 321–330.
42. Kayacan E, Ulutas B and Kaynak O. Grey system theory-based models in time series prediction. *Expert Syst Appl* 2010; 37: 1784–1789.
43. Wu H, Ye L-P, Shi W-Z, et al. Assessing the effects of land use spatial structure on urban heat islands using HJ-1B remote sensing imagery in Wuhan, China. *Int J Appl Earth Observ Geoinform* 2014; 32: 67–78.
44. Tsaur RC. Forecasting analysis by using fuzzy grey regression model for solving limited time series data. *Soft Comput* 2008; 12: 1105–1113.
45. Chang CJ, Li DC, Dai WL, et al. Utilizing an adaptive grey model for short-term time series forecasting: a case study of wafer-level packaging. *Math Probl Eng* 2013; 2013: 526806.
46. Wang J, Ma X, Wu J, et al. Optimization models based on GM (1, 1) and seasonal fluctuation for electricity demand forecasting. *Int J Electr Power Energ Syst* 2012; 43: 109–117.
47. Wu H, Sun Y, Shi W, et al. Examining the satellite-detected urban land use spatial patterns using multidimensional fractal dimension indices. *Remote Sens* 2013; 5: 5152–5172.
48. Amore M, Bonaccorso A, Ferrari F, et al. Eolo: software for the automatic on-line treatment and analysis of GPS data for environmental monitoring. *Comput Geosci* 2002; 28: 271–280.
49. Gresil M, Yu LY, Giurgiutiu V, et al. Predictive modeling of electromechanical impedance spectroscopy for composite materials. *Struct Health Monit* 2012; 11: 671–683.
50. Nagelkerke NJ. A note on a general definition of the coefficient of determination. *Biometrika* 1991; 78: 691–692.
51. Cameron AC and Windmeijer FA. An R-squared measure of goodness of fit for some common nonlinear regression models. *J Econom* 1997; 77: 329–342.
52. Wu H, Tao J, Li X, et al. A location based service approach for collision warning systems in concrete dam construction. *Safety Sci* 2013; 51: 338–346.